Available online at www.sciencedirect.com
SCIENCE DIRECT®
Optics Communications xxx (2006) xxx–xxx
OPTICS COMMUNICATIONS
www.elsevier.com/locate/optcom

# Absorption spectrum of rubidium and cesium dimers by compact computer operated spectrometer

S. Vdović [a,*], D. Sarkisyan [b], G. Pichler [a]

[a] Institute of Physics, Bijenička 46, P.O. Box 304, HR-10001 Zagreb, Croatia
[b] Institute for Physical Research, NAS of Armenia, Ashtarak-2, 378410, Armenia

Received 13 April 2006; received in revised form 6 June 2006; accepted 26 June 2006

**Abstract**

In this paper we are presenting the visible absorption spectrum of both rubidium and cesium vapor in the 570–870 K temperature range. We used a classical absorption spectroscopy experimental scheme with several new features. The first concerns the use of modern, compact, computer operated spectrometer (Ocean Optics HR4000CG-UV-NIR), which allowed us to record spectra instantaneously resulting in higher signal-to-noise ratio. The second improvement is connected with the use of the all-sapphire cells (ASC) enabling work with a high density of alkali atoms within precisely defined vapor column. In the superheated regime (above 700 K) thermal destruction of dimer molecules clearly distinguishes triplet from singlet transitions.


*PACS:* 33.20.Kf; 32.70.Jz; 34.20.Cf; 33.70.Fd; 33.70.−w

## 1. Introduction

Rubidium and cesium molecular and satellite bands in the visible spectral range are well known from numerous experimental [1,2] and theoretical [3–5] studies. In an absorption experiment, dimer absorption bands usually overlap with the far wings of the self-broadened atomic lines. In order to experimentally decrease the intensity of molecular bands, thermal destruction of dimer molecules must be achieved. Diminishing of molecular bands enables clear observation of the free–free and free–bound spectral transitions, which form the quasistatic wings [6] of spectral lines. Using an all-sapphire cell (ASC) with sapphire windows having optical axis perpendicular to the surface filled with small amount of cesium, it is possible to achieve the superheating regime [7,8]. At some critical temperature, depending upon the amount of the inserted cesium, the liquid cesium evaporates entirely and only the metal vapor, consisting of atoms and molecules, is present in cell. With a further increase of the cell temperature, the number of molecules decreases due to the increasing rate of collisional dissociation. In such an overheated atomic vapor, it is possible to observe satellite bands of atomic lines, which are completely hidden by strong molecular bands stemming from singlet transitions at lower temperatures [9]. A second, T-shaped, ASC contained pure rubidium and was not designed for work in superheating regime.

## 2. Experiment

The cesium vapor was generated in the 160 mm long sealed-off cylindrical ASC. The temperature of the vapor was measured with a thermocouple placed at the center of the outer wall of the ASC. Due to the small quantity of cesium ($m \approx 6$ mg) in the cell, at the temperature of $T_0 = 695$ K the whole amount of cesium is evaporated, with a vapor density of $N_{Cs}\,(T = 695\ \text{K}) = 3.5 \times 10^{17}\ \text{cm}^{-3}$ [10] which increases further with the temperature rise due to the thermal destruction of cesium molecules. The cell was heated in the specially designed linear oven and operated in 570–870 K temperature range.

* Corresponding author. Tel.: +385 14698858; fax: +385 14698889.
*E-mail address:* silvije@ifs.hr (S. Vdović).

0030-4018/$ - see front matter © 2006 Published by Elsevier B.V.
doi:10.1016/j.optcom.2006.06.070

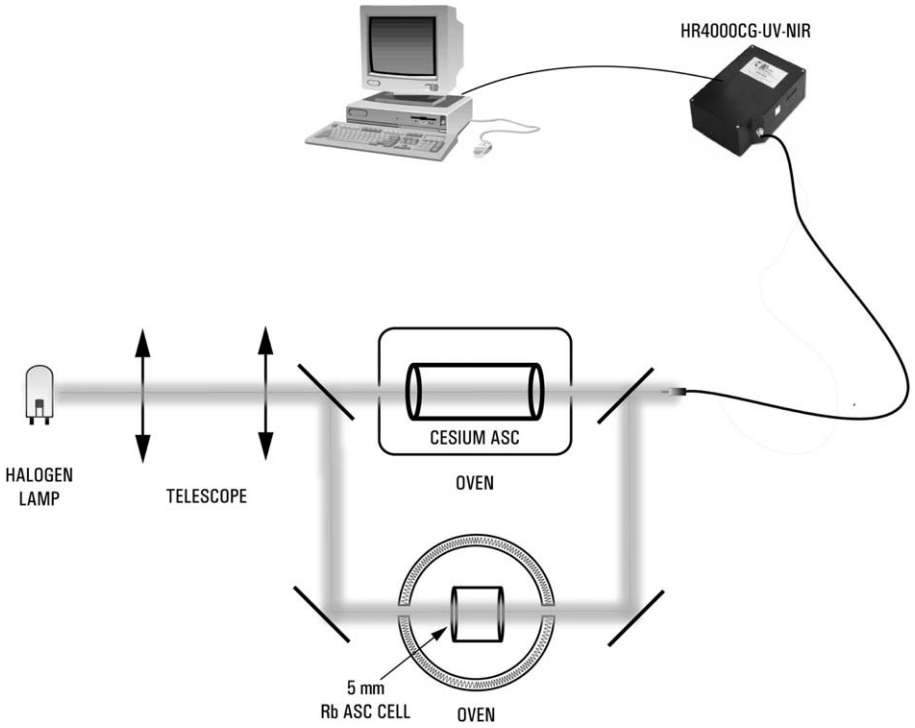


Fig. 1. Experimental apparatus.

The rubidium vapor was generated in the sealed-off T-shaped, 5 mm long, ASC. It was heated in the specially designed oven using two heaters, one for the body of the ASC and another for the side arm which served as a rubidium reservoir. In order to avoid condensation of the rubidium vapor at the windows of the ASC the body temperature had to be kept higher than the side arm temperature. We recorded spectra at temperatures ranging from 602 to 685 K because of the ASC temperature limit of approximately 750 K imposed by the use of low temperature glue in the fabrication process. These spectra are presented in Figs. 6 and 7.

The white light from a halogen lamp passing through the hot vapor was spectrally resolved and detected with an Ocean Optics HR4000CG-UV-NIR spectrometer (Fig. 1). The entrance aperture of the spectrometer was a 5-μm wide slit. The spectrometer utilizes a HC-1 Landis grating (300 lines per nanometer) designed to provide a 200–1100 nm wavelength range. The spectra are detected with a 3648-element linear silicon CCD array. This configuration results in 0.75 nm FWHM spectral resolution. The spectrometer was operated from a computer using the appropriate commercial software and the spectra were stored on a PC for later analysis.

## 3. Results

### 3.1. $Cs_2$

We shall first concentrate on the cesium dimer absorption spectrum since in this case the superheating mode that we worked in allowed us to observe almost all spectral features; first and multiple order resonance lines, singlet and triplet molecular bands as well as the various satellite bands. The linear absorption coefficient behavior is presented in Figs. 2–5 divided into two wavelength intervals for two different regimes: the case in which vapor temperatures are equal or below $T_0$ and the superheating regime.

Starting from shorter wavelengths (Figs. 2 and 4), the first resolved lines in the cesium spectra are the fourth cesium principal series doublet at 361.1 and 361.7 nm involving the $6S_{1/2} \rightarrow 9P_{3/2,1/2}$ transitions. At 387.6 and 388.9 nm the third cesium principal series doublet appears, corresponding to the $6S_{1/2} \rightarrow 8P_{3/2,1/2}$ transitions. An interesting feature is the band centered around 395 nm which is identified [11] as two molecular bands centered at 395.4 and 397.7 nm showing temperature dependence typical for the $Cs_2$ $1(X)^1\Sigma_g^+$ ground electronic state. Therefore we identified this spectral band as the absorption from the $Cs_2$ $X^1\Sigma_g^+$ state to one or more excited $Cs_2$ singlet state(s) which are connected with atomic asymptote $6s + 6d$ or even higher. The $Cs_2$ absorption band peaking at 420 nm consists of several singlet transitions from the $1(X)^1\Sigma_g^+$ state [11]. The second cesium principal series doublet at 455.5 and 459.3 nm is nicely seen at the beginning of the $Cs_2$ $1(X)^1\Sigma_g^+ \rightarrow 3(E)^1\Sigma_u^+$ molecular band centered at 480 nm. In the blue wing of the Cs 455.5 nm line the broad ion-pair satellite band is clearly pronounced stemming from the photoassociation of two ground state Cs atoms into long-range potential wells [7]. The satellite band peaking at 472 nm was observed only when the cesium dimer concen-

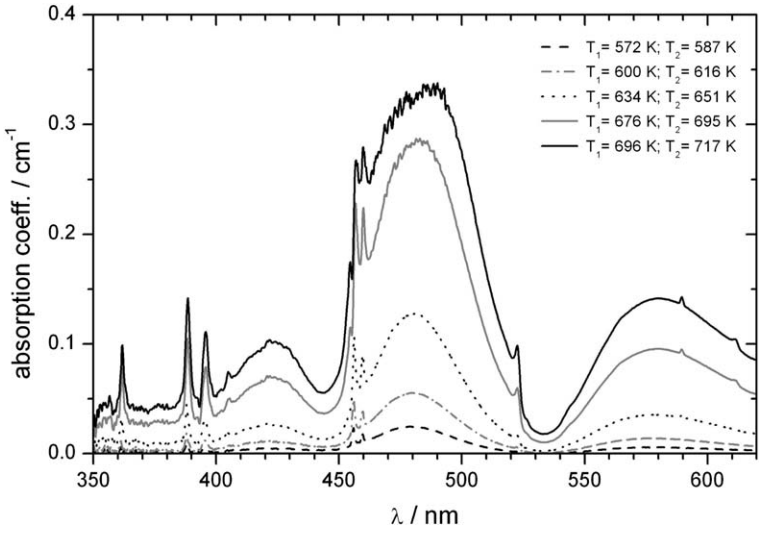


Fig. 2. Absorption coefficient in the 350–620 nm range of cesium vapor in a 160 mm long sapphire cell at increasing temperatures but below the critical temperature.

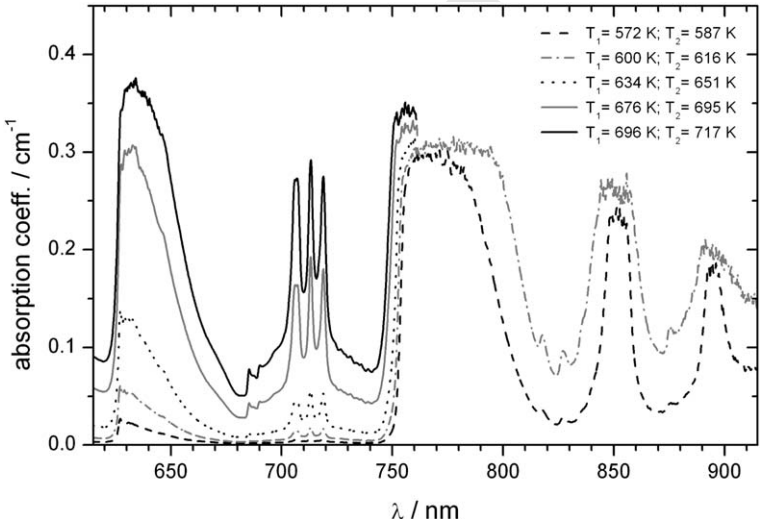


Fig. 3. Absorption coefficient in the 615-915 nm range of cesium vapor in a 160 mm long sapphire cell at increasing temperatures but below the critical temperature. Higher temperature spectra are not displayed above 760 nm due to high optical thickness of the medium in that range.

tration was reduced due to thermal destruction, above 770 K (see Fig. 4). This satellite band is predominantly formed by photoassociation (free → bound transitions). Located at the beginning of the X → E molecular band, at 522.5 nm and 526.4 nm, two satellite bands show no temperature dependence. The $Cs_2$ $1(X)^1\Sigma_g^+ \rightarrow 2(D)^1\Sigma_u^+$ absorption band is observed in the 530–620 nm spectral region and is overlapped with a $Cs_2$ band peaking at 611.5 nm which stems predominately from the free–bound $Cs_2$ $1(X)^1\Sigma_g^+ \rightarrow 3\,^1\Sigma_u^+$ transition [12]. The 589 nm feature is attributed to the sodium impurity D lines which appear in both cesium and rubidium spectra.

At longer wavelengths (Figs. 3 and 5), the X → C molecular band is formed in the 620–685 nm spectral region and is followed by the $1(X)^1\Sigma_g^+ \rightarrow 2(B)^1\Pi_u$ band in 750–800 nm interval which is optically thick at higher temperatures and is therefore not shown in the high temperature spectra (Fig. 5). Forbidden atomic 6s → 5d lines at 684.9 and 689.5 nm are placed next to the cesium diffuse band involving triplet transitions $1(a)^3\Sigma_u^+ \rightarrow 2^3\Pi_g(0_g^{+,-}, 1_g, 2_g)$ at 706.5, 713.2 and 718.8 nm [13]. This band shows no temperature dependence, consistent with the fact that the lowest triplet ground state has a very shallow potential so that photoassociation is the dominating mechanism in formation of the band. In addition to the self-broadened atomic lines of the first cesium principal series doublet, the features at 817, 827 and 835 nm are attributed to the cesium blue satellite bands identified as $1^3\Pi_g(2_g, 1_g, 0_g^+, 0_g^-) \leftarrow a^3\Sigma_u^+(1_u, 0_u^+)$ transitions

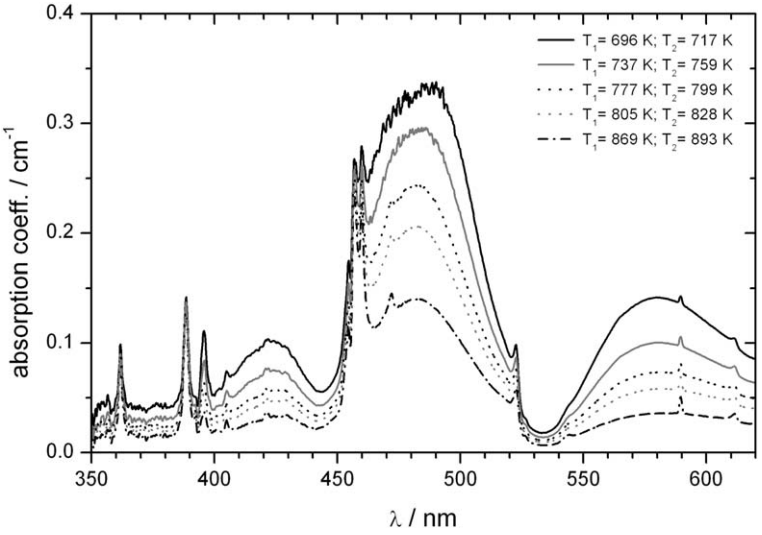


Fig. 4. Absorption coefficient in the 350–620 nm range of cesium vapor in a 160 mm long sapphire cell at increasing temperatures but above the critical temperature.

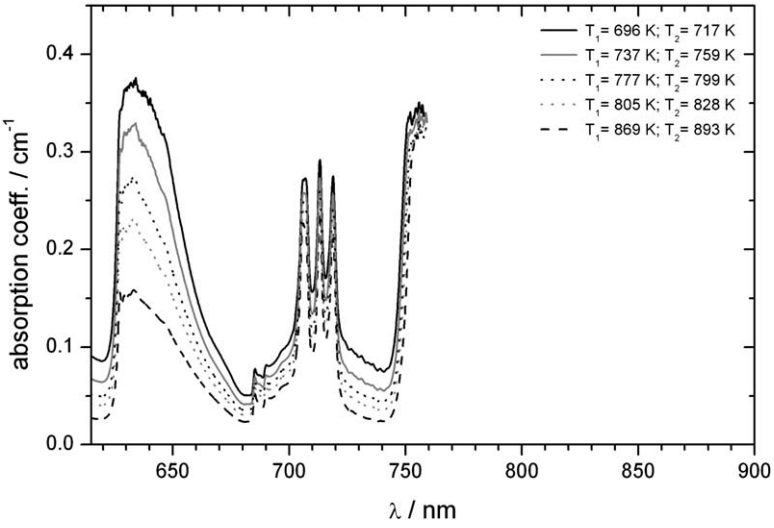


Fig. 5. Absorption coefficient in the 615–760 nm range of cesium vapor in a 160 mm long sapphire cell at increasing temperatures but above the critical temperature.

where the upper state dissociates into the $6^2P_{3/2} + 6^2S_{1/2}$ atomic asymptote [9]. The feature at 875.2 nm is attributed to the cesium satellite band stemming from the $Cs_2$ $0_g^+$ $(6^2S_{1/2} + 6^2P_{1/2})$ state [14].

### 3.2. $Rb_2$

The rubidium dimer absorption spectrum is divided in two spectral intervals and shown in Figs. 6 and 7. Atomic features are represented by the third (~360 nm), the second (~420 nm) and the first (780 and 795 nm) rubidium principal series doublet transitions. The 5s → 6p transitions near 420 nm coincide with the broad $Rb_2$ X → E band centered at 430 nm. Next to the X → E band, X → D band, the $1(X)^1\Sigma_g^+ \rightarrow 3(D)^1\Pi_u$ band occurs, peaking at 475 nm [15]. The last important feature in Fig. 6 is the rubidium diffuse band having three peaks at 601, 603 and 605.5 nm resulting from the $1(a)^3\Sigma_u^+ \rightarrow 2^3\Pi_g$ free–free and bound–free triplet transitions [15].

In Fig. 7 we present the absorption coefficient of rubidium vapor in the 640–930 nm range and the explanation of the most pronounced atomic and molecular spectral features now follows. The $1(X)^1\Sigma_g^+ \rightarrow 1(B)^1\Pi_u$ molecular band spreading from 640 to 730 nm is almost completely saturated. Triplet satellite bands originating from the $Rb_2$ long-range $1(a)^3\Sigma_u^+(0_u^-, 1_u) \rightarrow 1^3\Pi_g(2_g, 1_g, 0_g^\pm)$ transitions [16] are observed in the 740–750 nm wavelength range. The spectral shoulder appearing around 765 nm is connected with the $Rb_2$ $1(a)^3\Sigma_u^+(1_u) \rightarrow 1^3\Pi_g(0_g^+)$ transition, one of the well-known [16] triplet satellite bands. The

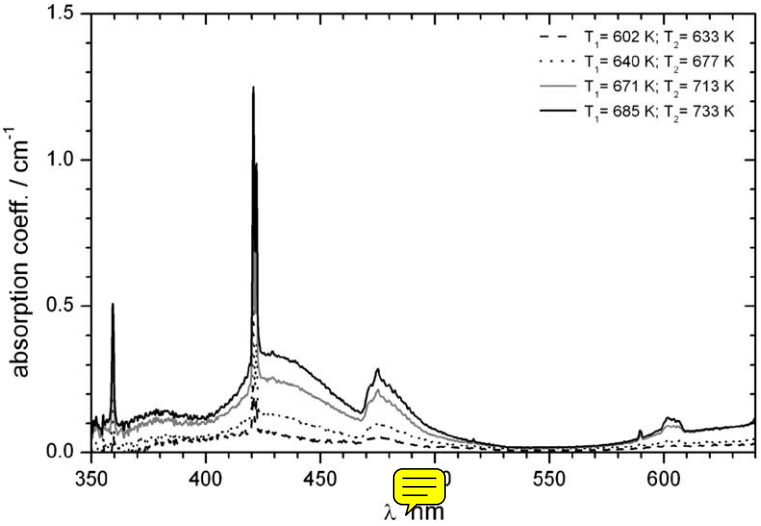


Fig. 6. Absorption coefficient of rubidium vapor in a 5 mm sapphire cell at increasing temperatures in the 350–640 nm spectral range. The rubidium resonance lines are self-broadened and saturated at higher temperatures leading to an incorrect calculated absorption coefficient which would normally be infinitely large at the resonance position. That is why spectra at higher temperatures (starting from $T_1 = 634$ K) are cut at 760 nm.

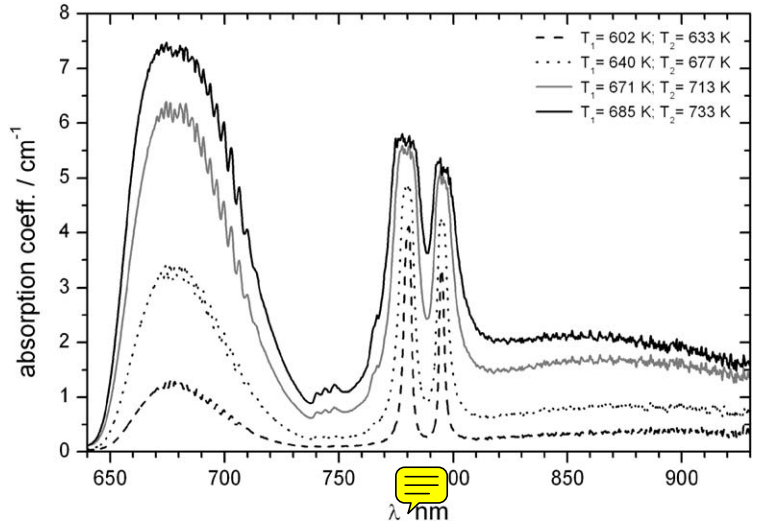


Fig. 7. Absorption coefficient of rubidium vapor in a 5 mm sapphire cell at increasing temperatures in the 640–930 nm spectral range. The spectra in the 760–915 nm range are omitted for the reasons stated in the caption of Fig. 6.

potassium D2 line at 766.7 nm is also visible. At wavelengths above 810 nm the undulations from bound–bound $Rb_2$ $1(X)^1\Sigma_g^+ \rightarrow 1(A)^1\Sigma_u^+$ transitions are observable.

## 4. Discussion

At present we shall not give any additional theoretical simulation since there is ongoing work toward complete ab initio calculations of potential curves and important transition dipole moments. However, the present data may serve as a first check of the quality of the potential curves and transition dipole moments obtained.

Some weakly resolved spectral appearances still deserve comments in both the $Rb_2$ and $Cs_2$ cases. In Figs. 2, 4 and 5 the absorption coefficients in the UV spectral region below 400 nm are not accurately evaluated since the halogen lamp is very weak in this spectral region. Because of that, in the near future we intend to use powerful (up to 100 mW) UV LEDs to make more reliable intensity measurements in this spectral region. This will, at least partly, exclude the influence of the stray light stemming from the visible part of the halogen lamp spectrum.

In Fig. 7 at the highest temperatures, above the critical temperature, a band at 695 nm can be clearly seen. It most probably stems from transitions at large interatomic separations, but it cannot be discerned whether it stems from the singlet or triplet manifold.

Finally, we would like to comment the critical temperature $T_0$ mentioned in measurements with our cesium cell. A simple technique based on an ASC filled with a

determined quantity of Cs metal could be a convenient tool for detection of chemical reaction of hot cesium vapor with other metals. Vapor of Cs dimers strongly absorb the radiation of the widely used He–Ne laser. Since the dimer concentration has a maximum at the temperature $T_0$, it is obvious that the transmission of the He–Ne laser at 632.8 nm will have a well-pronounced minimum at this temperature. If there is a slow chemical reaction of Cs atoms with materials used for the cell fabrication (including glue) this well-pronounced minimum will be shifted toward lower temperatures. In particular, when a small titanium strip (getter) has been inserted inside the sealed-off ASC, during several days of heating procedure at $T > 500\,^{\circ}\mathrm{C}$ a slow chemical reaction between Cs and Ti atoms was detected (there is formation of a so-called intermetallic compound). However, there is no chemical reaction between hot Cs atoms and the sapphire walls of ASC, even at $T \sim 800\,^{\circ}\mathrm{C}$. This simple technique can allow one to detect whether there is a chemical reaction of hot Cs vapor (or any other alkali metal) with any metal inserted beforehand into the sealed-off ASC.

## 5. Conclusion

Our principal aim was to show how useful a compact spectrometer can be in obtaining absorption spectrum over a wide spectral region, from the near UV, through the visible and into the near IR. The data on $Rb_2$ and $Cs_2$ are mostly well known, although some of the spectral features are still not entirely interpreted in terms of the corresponding potential curves and relevant transition dipole moments. However, we believe that present data may serve for further development of the understanding of alkali vapor absorption at high densities. This may serve in further application to high pressure pulsed light sources for special or general use.

## Acknowledgements

We acknowledge the support from the Ministry of Science and Technology of Republic of Croatia (Projects 0035002), the European Commission Research Training Network (FW-5) and the Alexander von Humboldt Foundation (Germany). D.S. acknowledges the support from Swiss SCOPES program (Grant IB 7320-110684/1).

## References

[1] R. Gupta, W. Happer, J. Wagner, E. Wennmyr, J. Chem. Phys. 68 (1978) 799.
[2] Č. Vadla, R. Beuc, V. Horvatić, M. Movre, A. Quentmeier, K. Niemax, Eur. Phys. J. D 37 (2006) 37.
[3] S.J. Park, S.W. Suh, Y.S. Lee, G.-H. Jeung, J. Mol. Spectrosc. 207 (2001) 129.
[4] F. Spiegelmann, D. Pavolini, J.-P. Daudey, J. Phys. B – At. Mol. Opt. Phys. 22 (1989) 2465.
[5] N. Spies, Ph.D. thesis, Universität Kaiserslautern;
W. Meyer, N. Spies, 1989, ~~in press~~
[6] D.H. Sarkisyan, A.S. Sarkisyan, A.K. Yalanusyan, Appl. Phys. B 66 (1998) 241;
D. Sarkisyan et al., Appl. Phys. B 70 (2000) 351.
[7] T. Ban, H. Skenderović, R. Beuc, I. Krajcar Bronić, S. Rousseau, A.R. Allouche, M. Aubert-Frécon, G. Pichler, Chem. Phys. Lett. 345 (2001) 423.
[8] T. Ban, D. Aumiler, G. Pichler, Phys. Rev. A 71 (2005) 022711.
[9] D. Veža, R. Beuc, S. Milošević, G. Pichler, Eur. Phys. J. D 2 (1998) 45.
[10] A.N. Nesmeyanov, Vapor Pressure of Elements, Academic Press, New York, 1963.
[11] T. Ban, H. Skenderović, S. Ter-Avetisyan, G. Pichler, Appl. Phys. B 72 (2001) 337.
[12] T. Ban, S. Ter-Avetisyan, H. Skenderović, R. Beuc, G. Pichler, Chem. Phys. Lett. 313 (1999) 110.
[13] G. Pichler, S. Milošević, D. Veža, R. Beuc, J. Phys. B – At. Mol. Phys. 16 (1983) 4619.
[14] R. Beuc, H. Skenderović, T. Ban, D. Veža, G. Pichler, W. Meyer, Eur. Phys. J. D 15 (2001) ~~15~~
[15] T. Ban, D. Aumiler, R. Beuc, G. Pichler, Eur. Phys. J. D 30 (2004) 57.
[16] M.-L. Almazar, O. Dulieu, F. Masnou-Seeuws, R. Beuc, G. Pichler, Eur. Phys. J. D 15 (2001) 355.